Available online at www.sciencedirect.com
SCIENCE DIRECT®
Catalysis Today 93–95 (2004) 163–171
CATALYSIS TODAY
www.elsevier.com/locate/cattod

The roles of redox and acid–base properties of silica-supported vanadia catalysts in the selective oxidation of ethane

Zhen Zhao [a,b,*], Yusuke Yamada [a], Atsushi Ueda [a], Hiroaki Sakurai [a], Tetsuhiko Kobayashi [a]

[a] *National Institute of Advanced Industrial Science and Technology (AIST), 1-8-31, Midorigaoka, Ikeda, Osaka 563-8577, Japan*
[b] *The State Key Laboratory of Heavy Oil Processing, Faculty of Chemical Science and Engineering, University of Petroleum Beijing, Xuefu Road, Changping, Beijing 102249, China*

Available online 6 August 2004

Abstract

The redox and acid–base characters of silica-supported vanadium or alkali-modified vanadium catalysts by varying vanadium loading were studied with the methods of H_2-TPR, NH_3-TPD and CO_2-TPD combining other structural characterization techniques of ESR, UV–vis spectroscopy. The effects of these properties on their catalytic performances for the ethane oxidation by oxygen were investigated. For both the unpromoted V/SiO_2 (V:Si = *x*:Si) and promoted Cs–V/SiO_2 (Cs:V:Si = 1:*x*:100) systems, the reduction extent and the reducibility increase with increasing vanadia loading and the presence of cesium enhances the reduction extent. The structures of the vanadyl species have large effect on the vanadia reducibility and the isolated surface vanadyl species are less reducible than the polymeric vanadyl species including microcrystalline vanadia. For the samples with high vanadia loading ($\geq$2.0%), the reducibility is high and thus the redox characteristic of the catalyst is one of the most important factors that govern the catalytic reactivity. In the samples with low vanadia loading (<0.5%), the reducibility is low. Therefore, the basicity or acidity characteristics of the catalyst become the major factors that control the catalytic reactivity. The cesium promoted samples Cs–V/SiO_2 (2.0 and 10.0%) exhibit high reducibilities, which qualitatively suggests that their oxygen mobility is very high and may result in deep oxidation of ethane. In contrast, those samples with low reducibility are selective for the oxidation of ethane including ODH to ethylene and oxygenate formation.

Keywords: Redox property; Acid–base characters; Silica-supported vanadium catalyst; Selective oxidation of ethane; Roles of redox and acid–base characteristics

1. Introduction

It has been generally recognized that the acid–base character and redox property are two of the important factors governing the catalysis of metal oxides [1–5]. These two factors are often dealt with separately in hydrocarbon oxidation catalysis. In the most cases the redox property is closely related to the catalytic activity, while the basic–acidic nature is usually related to the product selectivity.

There are many reports concerning the redox property by TPR/O and the relation between it and catalytic performance of vanadium-supported oxide catalysts in the past two decades [6–18]. However, there currently appears to be a lack of consensus among these publications as to the following points since the measurement conditions in TPR for different researchers were somewhat different [9]. For example, the supports (TiO_2, Al_2O_3, SiO_2, ZrO_2); the reducing gases (H_2, CO, NH_3, C_2H_6 or *n*-C_4H_{10}); the concentration of reducing gas; reduction temperature range and heating rate, etc.:

(a) The reduction degree of V^{5+}, i.e., $V^{5+} \rightarrow V^{4+}$ or $V^{5+} \rightarrow V^{3+}$. It is sure that V^{5+} can be reduced to V^{3+} when CO is used as reduction agent as one CO molecule remove one oxygen per V to form CO_2 [12,13]. However, the situation becomes complicated when H_2 is employed as reducing agent. Some researchers reported that V^{5+} was reduced to V^{3+} determined by the hydrogen consumption ratio per V (H/V) closing to 2 [14–16]. The others pointed out that V^{5+} only was reduced to V^{4+} un-

* Corresponding author. Tel.: +86-10-89731586; fax: +86-10-89731586.
E-mail address: zhenzhao@bjpeu.edu.cn (Z. Zhao).

0920-5861/$ – see front matter © 2004 Elsevier B.V. All rights reserved.
doi:10.1016/j.cattod.2004.06.130

der some conditions [10,17,18]. For example, Koranne et al. [18] did high resolution TPR study and found that for V_2O_5/Al_2O_3 the average oxidation state of V after reduction to 900 °C is consistent with the stoichiometry $V^{5+} \rightarrow V^{4+}$, whereas the V_2O_5/SiO_2 catalysts exhibited 70% reduction of the $V_2O_5 \rightarrow V_2O_3$ as did bulk V_2O_5. Similarly, Harber et al. [17] and Erdohelyi et al. [10] reported that V^{5+} was reduced to V^{3+} on TiO_2, while V^{5+} was only reduced to V^{4+} on SiO_2 and Al_2O_3.

(b) The reducibility order of different types of vanadyl species (containing isolated vanadyl species, polymeric species and V_2O_5 cluster). Recently, Arena et al. [16] studied the structure and dispersion of supported-vanadia catalyst by H_2-TPR. They indicated the ease of reduction follows the sequence: defective coordinatively unsaturated surface V ion $>T_d$ isolated vanadyls > bidimensional polymeric vanadyls > three-dimensional cluster or crystalline V_2O_5. On the contrary, very recently, Gao et al. [15] reported that the surface polymerized vanadia species are more easily reduced than isolated surface vanadia species in reducing environments (ethane or *n*-butane).

The catalytic performance of vanadium-supported catalyst can be altered by the addition of alkali metal as promoter. There are some papers concerning alkali metal modified vanadium-supported catalysts [19–26]. Generally, the presence of alkali metal induces a decrease of activity in oxidation reactions. The effect of alkali metal on the selectivity to the desired product may be positive or negative, depending on the type of reactant molecular, on the alkali/V ratio and reaction conditions. However, alkali promotion effect on the catalytic performance is not fully understood. The scarce reducibility data about alkali-modified vanadium-supported catalysts, obtained by TPR techniques, are also contradictory. Some researchers reported the increase in the temperature of the reduction peak maximum [20,24] or onset temperature [21] when alkali metal was added. This is generally considered as the reason to cause the decrease in activity [8,21,22,31]. The others showed that the decrease in the reduction peak maximum [27,28] or the increase in reduction extent by addition of alkali metal [27–30].

Very recently, we reported that silica-supported alkali metal and a small amount of Fe, V or Bi can catalyze the selective oxidation of ethane [32–39] to acetaldehyde and even to acrolein by gas-phase oxygen. Both the ethane conversion and total selectivity to aldehydes were enhanced by the addition of alkali metal during ethane oxidation. Although some roles of alkali metal have been classified [34–39], however, there are still some unknown points. In this work the redox property and acid–base nature of several systems of silica-supported vanadia catalysts with or without an alkali metal were studied and the effects of these characteristics on their catalytic performances for ethane oxidation were investigated.

2. Experimental

2.1. Catalyst preparation

All the catalysts were prepared by the impregnation method [35–38].

2.2. Activity measurement

A fixed bed flow reactor (quartz tube, 6 mm i.d.) was used at atmospheric pressure for the catalytic activity measurements. The activity measurement conditions and product analysis method were reported in detail elsewhere [32–37].

2.3. Characterization of catalysts

Specific surface areas were determined by the BET single-point method using a surface area analyzer (Quantachrom, Jr).

UV–vis absorption spectra of the samples were measured with a spectrophotometer (MCPD 2000, Otsuka Electric Co.) equipped with a multi-channel photo detector. The spectral resolution is 2 nm. SiO_2 was used as a reference sample.

Electron spin resonance (ESR) of the samples was measured in the X-band region by using a spectrometer (ESP-300E, Bruker) at liquid nitrogen temperature (−196 °C). Each sample (100 mg) was placed in a quartz tube in solid state.

Temperature-programmed reduction (TPR) of hydrogen was carried out with an automatic TPD system (Bell Japan, Inc). The sample (300 mg) was loaded in an U-type quartz tube and pretreated at 600 °C in flowing the mixed gases of 25% O_2 and 75% of helium for 1 h. After cooling in He flow to 50 °C, the He gas was switched to a 1% H_2/He mixed gases with a flow rate 30 ml/min. The temperature was then ramped to 850 °C, at a heating rate of 10 °C/min. The hydrogen signal was analyzed with an on-line quadrupole mass detector.

Temperature-programmed desorption (TPD) of CO_2 was conducted on the same apparatus used for TPR measurement. The sample (400 mg) was loaded in an U-type quartz tube and pretreated at 600 °C in flowing He for 1 h. After cooling to 50 °C the sample was saturated in a 25% CO_2/He mixture stream (30 ml/min) for 1 h at 50 °C and afterwards the sample was flushed under the He carrier flowing to room temperature. Finally the temperature was ramped to 600 °C, at a heating rate of 10 °C/min. The CO_2 signal was analyzed with an on-line quadrupole mass detector.

Temperature-programmed desorption (TPD) of NH_3 was also measured on the above apparatus. The sample (400 mg) was loaded in an U-type quartz tube and pretreated at 600 °C in flowing the mixed gas of 25% O_2 and 75% He for 1 h. After cooling to 150 °C the sample was saturated in a 25% NH_3/He mixture stream (30 ml/min) for 1 h at 150 °C and further for 1 h from 150 to 100 °C in flowing same mixed gases (25% NH_3/He). And afterwards the sample

was flushed under the He carrier flowing for 1 h at 100 °C. Finally, the temperature was then ramped to 500 °C, at a heating rate of 10 °C/min. The NH_3 signal was analyzed with an on-line quadrupole mass detector. For comparison, the measurements that NH_3 was adsorbed at 50 °C for 1 h, were also conducted.

3. Results and discussion

3.1. The structures of the catalysts

The dispersion and structures of V/SiO_2 (V:Si = x:100), and Cs–V/SiO_2 (Cs:V:Si = 1:x:100) (x = 0.0, 0.02, 0.05, 0.1, 0.5, 1.0, 2.0, 5.0, 10.0, 20.0) were studied and reported in our previous work [37]. The main results about the structure of these samples can be briefly summarized as follows. In both systems, isolated vanadyl species with tetrahedral coordination exist when vanadium loadings are very low (≤0.1 at.%), polymeric vanadyl species including vanadium–oxygen cluster and V_2O_5 microcrystalline are present when vanadium loadings are high (>5 at.%) which was identified by Raman spectra and will be reported in detail elsewhere [40]. In the medium loading of vanadium case, both polymeric vanadyl species and isolated vanadium species may exist or one type of species is predominate depend on the exact vanadium loading and presence or absence of cesium. Presence of cesium has no effect on the structure of samples with very low loading of vanadium, while it promotes the dispersion of vanadium on silica or makes some kind of alkali-vanadate [40], which makes the some octahedral coordinations change to tetrahedral ones ($0.1 \leq x \leq 2.0$).

3.2. Redox properties of the catalysts

H_2-TPR spectra of V/SiO_2 (V:Si = x:100, x = 0.1, 0.5, 2.0, 5.0 and 10.0) and Cs–V/SiO_2 (Cs:V:Si = 1:x:100, x = 0.1, 0.5, 2.0 and 10.0) are illustrated in Figs. 1 and 2, respectively. In both systems, only one reduction peak was observed in the spectra when vanadium loadings were equal to or less than 0.5%. This result may indicate that this peak is due to the reduction of V^{5+} to V^{4+} by hydrogen. When vanadium loadings were greater than 0.5% two and four reduction peaks were obtained in the spectra of V/SiO_2 and Cs–V/SiO_2 system, respectively.

The corresponding TPR results of these two series of samples (i.e., the initial reduction temperature (T_{onset}), the maximum reduction temperature (T_{max}), the total area of reduction peaks) are listed in Table 1. In both systems T_{onset} decreases with increasing vanadium loading indicating that the reducibility of surface vanadyl species increases with increasing vanadium content. In the spectra of V/SiO_2 system, T_{max} decreases with the increasing of vanadium loading and reach minimum at 2.0 at.%, then it increases with further increasing the vanadium loading. In the presence of

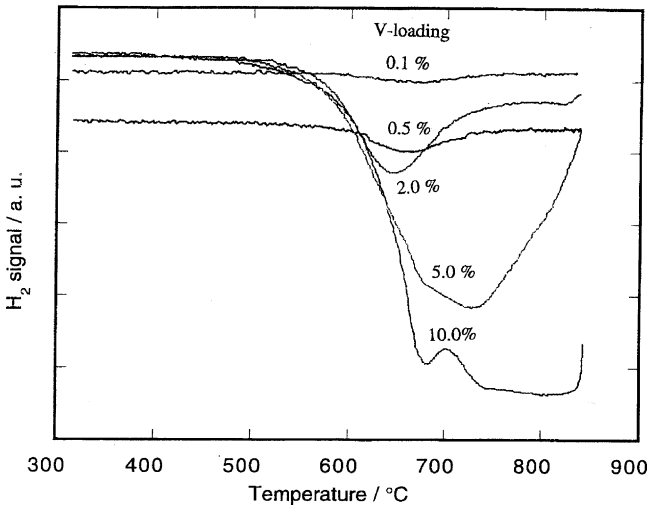

Fig. 1. H_2-TPR curves of V/SiO_2 (V:Si = x:100; x = 0.1, 0.5, 2.0, 5.0 and 10.0). Heating rate: 10 °C/min, 1% H_2, He balance.

cesium, i.e., in Cs–V/SiO_2 system, when vanadium loading ≤ 0.5%, T_{max} is higher by 30–50 °C than that in the case of V/SiO_2, while the area of reduction peak is much higher than that in V/SiO_2. When vanadium loading is equal to or greater than 2.0 at.%, two peaks at much lower temperature were observed besides the two peaks at high temperatures, which are similar to those in V/SiO_2. These two low temperature peaks must be caused by the interaction between cesium and vanadium. The presence of cesium promotes the interaction of different vanadium ions when vanadium loading is high (>2.0%) which will be discussed elsewhere [40] by ESR measurement. In Cs–V/SiO_2 (Cs:V:Si = 1:x:100) system, the ratio of Cs/V is less than 1.0 when vanadium loading is greater than 2.0%, i.e., not all the vanadium ions are close to the Cs ions. There are at least two types of vanadyl species existing in the samples with high vanadium loading. One type is vanadium ions near cesium, or some

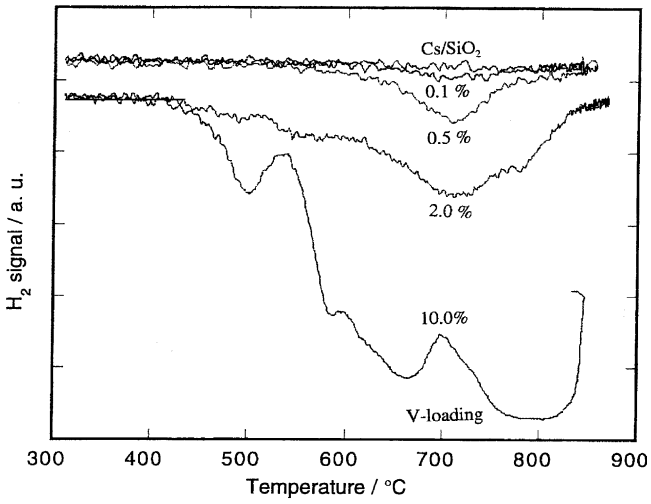

Fig. 2. H_2-TPR curves of Cs–V/SiO_2 (Cs:V:Si = 1:x:100; x = 0.0, 0.1, 0.5, 2.0 and 10.0). Heating rate: 10 °C/min, 1% H_2, He balance.

Table 1
TPR results of V/SiO_2 (V:Si = *x*:100) and Cs–V/SiO_2 (Cs:V:Si = 1:*x*:100)

	Vanadium loading (%)	Surface area (m^2/g)	T_{onset} (°C)	$T_{max}(1)$ (°C)	$T_{max}(2)$ (°C)	$T_{max}(3)$ (°C)	$T_{max}(4)$ (°C)	Total area of TPR peaks (a.u.)
V/SiO_2	0.1	388	563	683				0.4
	0.5	350	536	658				0.9
	2.0	346	498	647	830			4.3
	5.0	203	482	679	730			11.3
	10.0	47	479	681	785			17.9
Cs–V/SiO_2	0.1	158	599	711				1.0
	0.5	203	556	712				4.1
	2.0	108	426	491	549	716	783	10.9
	10.0	10	408	503	589	668	795	39.2

kinds of alkali vanadate formation [40]. The other is the vanadia far from cesium, which are similar to unpromoted ones. The strong interaction presents between the different vanadyl species in the former type. The interaction between the vanadyl species in latter type is weaker, which is similar to the case in V/SiO_2. Therefore, the first two peaks at lower temperature can be assigned to the reduction of the vanadyl species in former types, and the last two peaks at higher temperatures are assigned to the reduction of vanadyl species in the second type. The result that reduction maximum temperatures of last two peaks are similar to those in V/SiO_2 supports this assignment.

In order to further compare the reduction extent of the measured samples, the UV–vis and ESR spectra were recorded for the samples after TPR. For comparison, the UV–vis spectra for the some samples before TPR are also included.

UV–vis diffuse reflectance spectroscopy has been widely used to investigate the structures and oxidation states of vanadium-containing solid oxides that possess the ligand-to-metal charge transfer (LMCT) transition of V^{5+} in the region of 550–200 nm and d–d transitions of V^{4+} and V^{3+} in the range of 400–1000 nm [15]. In the region of 400–600 nm, the V ions with different valence (3+, 4+, and 5+) can exist. And it is also difficult to distinguish the V^{4+} and V^{3+} d–d electron transition band since these bands are located in the same range and tend to be broad and weak. However, V^{5+} can be distinguished from V^{4+} and V^{3+}. The bands 200–400 and 600–800 nm are the characteristic absorption bands for V^{5+} and V^{4+}/V^{3+}, respectively. Therefore, the ratio of the d–d electron transition band area of V^{4+}/V^{3+} (600–800 nm) to the area of LMCT band of V^{5+} (200–400 nm) was chosen as a parameter to relatively quantify the extent of reduction of V^{5+} cations in this study [15].

Figs. 3 and 4 show the UV–vis spectra for the used sample for TPR of V/SiO_2 (V:Si = *x*:100, *x* = 0.1, 0.5, 2.0, 5.0, and 10.0) and Cs–V/SiO_2 (Cs:V:Si = 1:*x*:100, *x* = 0.1, 0.5, 2.0, and 10.0), respectively. The ratio of absorption band area (600–800 nm) to the band area (220–400 nm) was calculated and listed in Table 2. It can be seen, from Figs. 3 and 4 and Table 2, that a very small amount of V^{4+}/V^{3+} present on the samples with medium or high vanadium loading before TPR, which is consistent with the ESR results [40]. In the case after TPR, the intensity of the LMCT band representing as V^{5+} decreases, while the intensity of d–d electron transition band standing for V^{4+}/V^{3+} increases. The ratio of the absorption band area (600–800 nm) to the band area (220–400 nm) is very small when vanadium loading is low indicating that a small fraction of V^{5+} was reduced to V^{4+}/V^{3+} during reduction. It increases with the increasing of vanadium loading suggesting that the extent of reduction increases with the increasing of vanadium loading. Furthermore, the presence of cesium the ratio of the absorption band area (600–800 nm) to the band area (220–400 nm) was larger than that in the

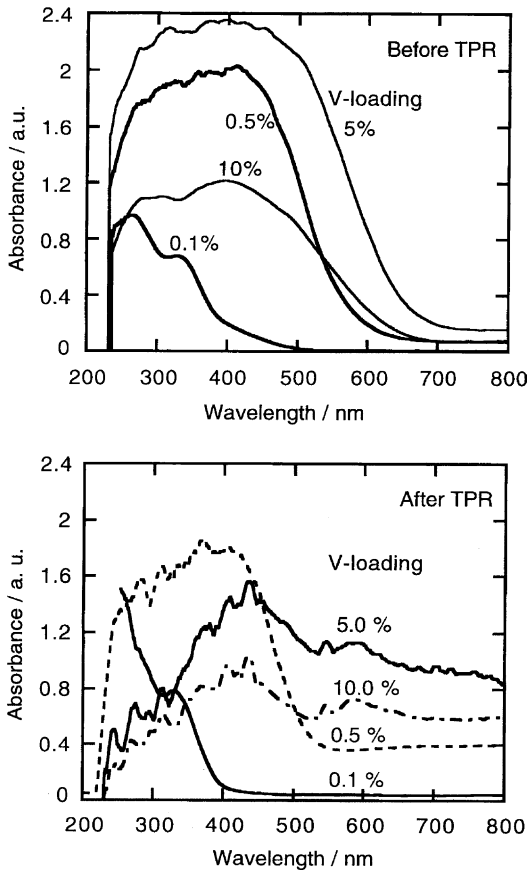

Fig. 3. UV–vis spectra of V/SiO_2 (V:Si = *x*:100) before and after H_2-TPR.

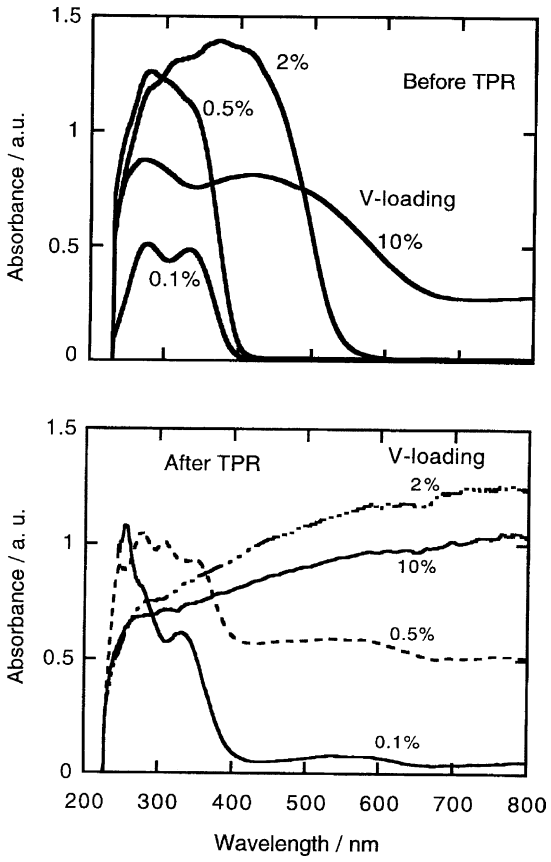

Fig. 4. UV–vis spectra of Cs–V/SiO_2 (Cs:V:Si = 1:*x*:100) before and after H_2-TPR.

case without cesium when vanadium loading is same. This result demonstrates that the presence of cesium increases the extent of reduction. This consideration is also confirmed by a higher ESR signal of V^{4+} for the sample with cesium after TPR. The similar phenomenon that the addition of potassium salts to V_2O_5 increased the extent of reduction of V_2O_5 was reported in previous study [27,28]. The two considerations that the extent of reduction was enhanced with the increasing of vanadium loading and presence of cesium is also supported by the color changes of the samples after TPR (in Table 2).

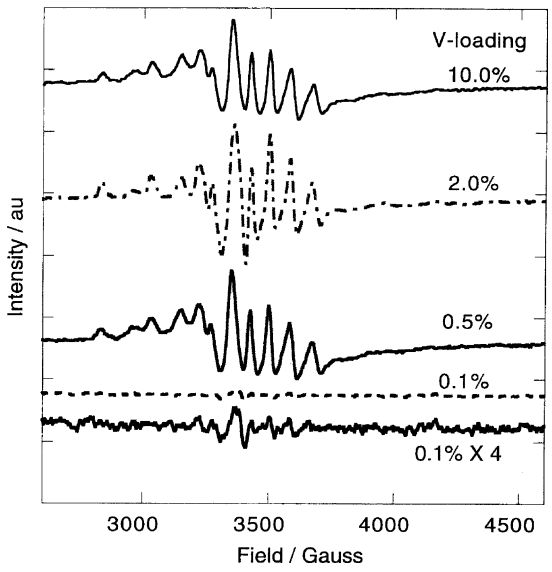

Fig. 5. ESR spectra of Cs–V/SiO_2 (Cs:V:Si = 1:*x*:100) after TPR.

The ESR spectra of Cs–V/SiO_2 (Cs:V:Si = 1:*x*:100, *x* = 0.1, 0.5, 2.0, and 10.0) after TPR are shown in Fig. 5. A very perfect hyperfine structure of V^{4+} was observed in the all spectra of the measured samples indicating that V^{5+} was mainly reduced to V^{4+}. As described above, in TPR profiles, ESR results further confirmed that a very small fraction of V^{5+} was reduced for the samples with low vanadium loading during reduction process, and the reduction extent increases with the increasing of vanadium loading.

The main features of the H_2-TPR results in this study could be summarized as follows:

(1) In both systems of V/SiO_2 and Cs–V/SiO_2, the reducibility increases with the increasing of vanadium loading amount according to the result that the initial temperature decreased with the increasing of vanadium content.
(2) In both systems, the reduction extents increase with the increasing of vanadium loading.

The two points above strongly suggest that the structures of the vanadyl species have large effect on the vanadia reducibility and the isolated surface vanadyl

Table 2
The color and the ratio of d–d electron transition band area of V^{4+}/V^{5+} (600–800 nm) to the area of LMCT band of V^{4+} (220–400 nm) of V/SiO_2 (V:Si = *x*:100) and Cs–V/SiO_2 (Cs:V:Si = 1:*x*:100) before and after TPR

Vanadium loading (%)		Before color	Ratio before TPR	After color	Ratio after TPR
V/SiO_2	0.1	Light yellow	0.0	White	0.07
	0.5	Orange	0.07	Orange	0.32
	2.0	Brick red		Deep green	
	5.0	Deep brick red	0.21	Dark green	1.30
	10.0	Brown	0.16	Dark green	1.27
Cs–V/SiO_2	0.1	White	0.0	Slight grey	0.11
	0.5	White	0.0	Grey	0.67
	2.0	Yellow	0.0	Black	1.95
	10.0	Brown	0.31	Black	1.93

species are less reducible than the polymeric vanadyl species including microcrystalline.

(3) The presence of cesium enhances the reduction extent of all the samples compared with the unpromoted samples with the same vanadium loading. However, the variation of the initial temperature and the maximum reduction temperature is complicated. For the samples with medium and high vanadium loading, both the initial temperature and maximum peak temperature for the first peak greatly decreased by the addition of cesium. This result indicates that the reducibility largely increases for the samples with high vanadium loading by the addition of cesium. For the samples with low vanadium loading ($\leq$0.5%), both the initial temperature and the maximum of peak temperature increased by the addition of cesium.

(4) Only one reduction peak was observed on the sample with low vanadium loading ($\leq$0.5%), which was mainly attributed to the reduction of V^{5+} to V^{4+}. Two reduction peaks were observed on the samples with medium or high vanadium loading ($\geq$2.0%) which are due to different type of polymeric vanadyl species reduction. In general, V_2O_5 is also a kind of polymeric vanadyl species.

During TPR process, not only were the metallic cations with high valence reduced to the ions with low valence or metal atoms by H_2 or CO, but also the lattice oxygen ion (O^{2-}) involved the process due to H_2O and CO_2 formed. Therefore, the following information can be also reflected by TPR measurement:

(a) The reducibility of metallic ion with high valence to the ion with low valence or metal atom.
(b) The potential to remove or take up oxygen [27], i.e., the mobility of lattice oxygen.
(c) The stability of the oxide or supported oxide against the reducing atmosphere or gases.

For the samples V/SiO_2 with relatively low vanadium loading (0.1–1.0%), the addition of cesium promoted the transformation of some polymeric vanadyl species with octahedral coordination to isolated ones with tetrahedral coordination and thus both initial temperature and maximum peak temperature were enhanced. For the samples V/SiO_2 with high vanadium loading ($\geq$2.0%), the interaction of different vanadyl species increased by the addition of cesium and some kind of cesium-vanadate formed [40], thus the reducibility was enhanced.

In both systems of V/SiO_2 and $Cs–V/SiO_2$ the bandgap energy, as reported in our previous work [37], decreased with the increasing of vanadium loading, which bring about the delocalization of electrons and, hence, the higher redox property. The bandgap energy of $Cs–V/SiO_2$ is higher than that of V/SiO_2 when vanadium loading is medium or low, while the bandgap energy of $Cs–V/SiO_2$ is lower than that of V/SiO_2 when vanadium loading is high. These results are in agreement with the TPR results.

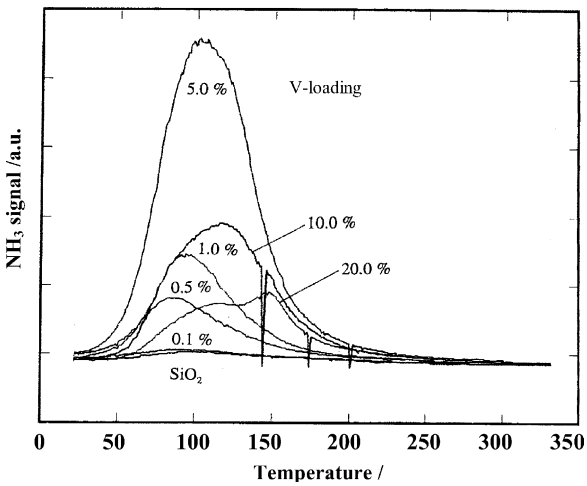

Fig. 6. NH_3-TPD curves of V/SiO_2 (V:Si = x:100; x = 0.0, 0.1, 0.5, 1.0, 5.0, 10.0 and 20.0).

3.3. The acidity and basicity of catalyst

The acidity of the catalyst was measured by NH_3-TPD, and the basicity of the catalyst was evaluated by CO_2-TPD. Fig. 6 depicts the NH_3-TPD profiles of V/SiO_2 (V:Si = x:100, x = 0.0, 0.1, 0.5, 1.0, 5.0, 10.0, and 20.0). The corresponding results are shown in Table 3. A very small desorption peak of ammonia was detected on the bare SiO_2. The desorption amount of NH_3 was enhanced by the introduction of V on silica. And the desorption amount of NH_3 per square metre (A_d/A_s) increases with increasing vanadium loading indicating that vanadyl species possess acid site on silica. Moreover, the maximum temperature for NH_3 desorption increases with the increasing of vanadium loading and for the samples with high vanadium loading (10.0, 20.0%) the second peak appeared at high temperature. This result suggests that the strength of acidity increases with the increasing of vanadium loading. The maximum of desorption temperature is relatively low indicating that vanadyl species provide weak acidic site. On the other hand, it may contain some amount of physical adsorption of NH_3 due to the adsorption of NH_3 at low temperature (50 °C). However, it mainly reflect the weak chemical adsorption of NH_3 due to no relation between the adsorption and the surface area, but it only related to the density of vanadyl species.

CO_2-TPD curves of $Cs–V/SiO_2$ (Cs:V:Si = 1:x:100, x = 0.0, 0.1, 0.5, 2.0, 10.0) are shown in Fig. 7. When the ratio of Cs/V is higher than 1.0, a large CO_2 desorption peak was observed, while a very weak CO_2-desorption peak was obtained when the ratio of Cs/V is less than 1.0. This result further supported that vanadyl species provide acidic site on silica and cesium oxide possesses basic role.

The main characters of NH_3-TPD and CO_2-TPD results could be summarized as follows.

Bare silica has very low density of acidity and basicity due to very small peaks were observed on both NH_3-TPD and CO_2-TPD. The acidic density increased by the addition

Table 3
NH_3-TPD results of V/SiO_2 (V:Si = *x*:100)

Vanadium loading (%)	Surface area (m^2/g)	*T*(1) (°C)	*T*(2) (°C)	Total area of desorption peaks (cm^2)	S_d/S_a[a] ($\times 10^{-3}$)
SiO_2	396	88		0.59	1.49
0.1	388	86		0.96	2.47
0.5	350	85		4.93	14.08
1.0	354	95		6.73	19.01
5.0	203	103		23.64	116.46
10.0	47	118	150	11.22	238.72
20.0	15	112	148	4.95	330.00

[a] S_d: total area of desorption peaks in NH_3-TPD; S_a: surface area; S_d/S_a: total areas of desorption peaks divided by the corresponding surface area.

of vanadium on silica indicates that vanadium play an acidic site on silica. The acidity and basicity can be altered by the addition of alkali metal. In Cs–V/SiO_2 (Cs:V:Si = 1:*x*:100) system, CO_2-TPD peak area and the maximum of peak temperature decreased with the increasing of vanadium loading further suggests that vanadium site in SiO_2 play a role of acidic site. It is because that the presence of vanadium neutralized the basic site of alkali metal oxide.

3.4. The effect of vanadium loading amount on the catalytic performance of V/SiO_2 (V:Si = x:100) and Cs–V/SiO_2 (Cs:V:Si = 1:x:100)

The catalytic performances of these two series of V/SiO_2 and Cs–V/SiO_2, as reported in our previous work [37], can be briefly summarized as follows.

Three different catalytic properties in the product selectivity were observed, the aldehyde formation, the oxidative dehydrogenation, and combustion, depending upon the vanadium loading amount and the presence or the absence of cesium. Very low loading of vanadium (V:Si = 0.02–0.1 at.%) and the addition of Cs (Cs:Si = 1 at.%) on silica were found to be important for the formation of aldehyde. Not only acetaldehyde but also acrolein was observed in the aldehyde formation from ethane. On the other hand, catalysts with medium and high vanadium loadings (V:Si = 0.5–20 at.%) gave a dehydrogenated product, ethylene, when Cs was not added to the catalysts. The cesium addition to the catalysts with medium and high vanadium loadings altered the catalytic property from ODH to combustion.

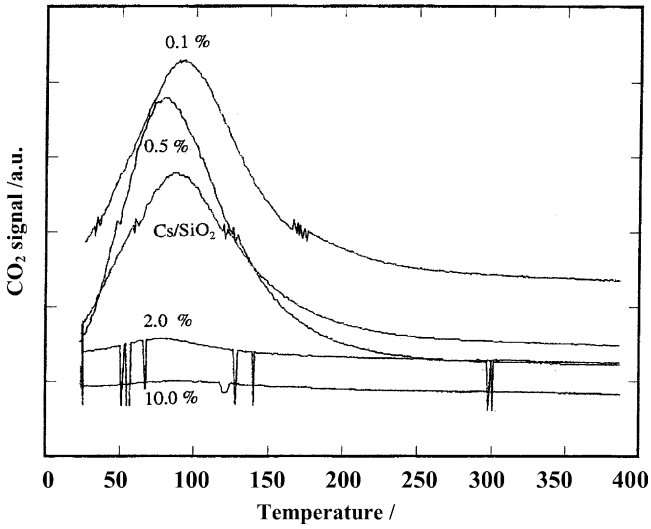

Fig. 7. CO_2-TPD curves of Cs–V/SiO_2 (Cs:V:Si = 1:*x*:100; *x* = 0.0, 0.1, 0.5, 2.0 and 10.0).

3.5. The relations between reducibility, acid–base properties and catalytic performances

The relation between ethane conversion per square metre of V/SiO_2 (V:Si = *x*:100) and Cs–V/SiO_2 (Cs:V:Si = 1:*x*:100) and their initial temperature in H_2-TPR are described in Figs. 8 and 9, respectively. In V/SiO_2 system, the ethane conversion monotonously increased with the decreasing of the initial temperature in H_2-TPR indicating that the reducibility of V/SiO_2 is an important factor to govern their reactivities. In the system of Cs–V/SiO_2 (Cs:V:Si = 1:*x*:100), a rough correlation between the reducibility and their reactivity was observed demonstrating that may present other factors to control the activity besides the reducibility.

In the presence of cesium, the samples with high vanadium loading (≥2.0%) are very active for ethane conversion, but they are for deep oxidation. At same time their reducibility are much higher than others. Therefore, the catalysts possessing much high reducibility, i.e., their oxygen mobility are very high, are for deep oxidation of hydrocarbon. The other samples whose reducibilities are much lower than the samples of Cs–V/SiO_2 (2.0 and 10.0%). At the same time they have the catalytic property for ODH over V/SiO_2 and for oxygenate formation over Cs–V/SiO_2. The catalyst whose reducibility or oxygen mobility is not so high is favorable for the selective oxidation including ODH of ethane and oxygenate formation. The reason why addition of cesium the catalytic performance of V/SiO_2 (≥2.0%) was changed from ODH to deep oxidation was given herein. The reducibility of supported catalysts not only relates to their reactivity, but also controls the product distribution in some cases.

In V/SiO_2 (V:Si = *x*:100) system, the acidic density increased with the increasing vanadium loading. Same trend was observed about the selectivity to ethylene on the dependence of vanadium loading. These results demonstrate

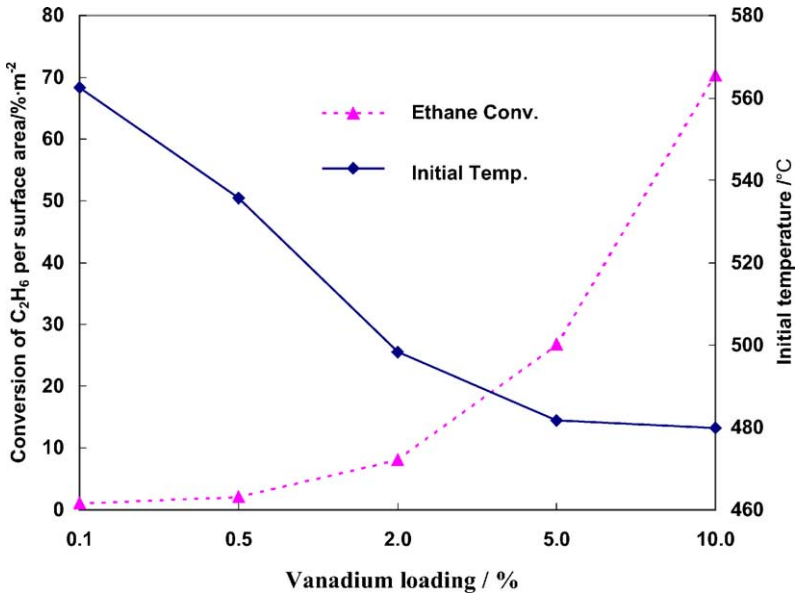

Fig. 8. Relation between ethane conversion per unit surface area of V/SiO_2 and its initial temperature in H_2-TPR. The reaction temperature for $C_2H_6 + O_2$ is 475 °C.

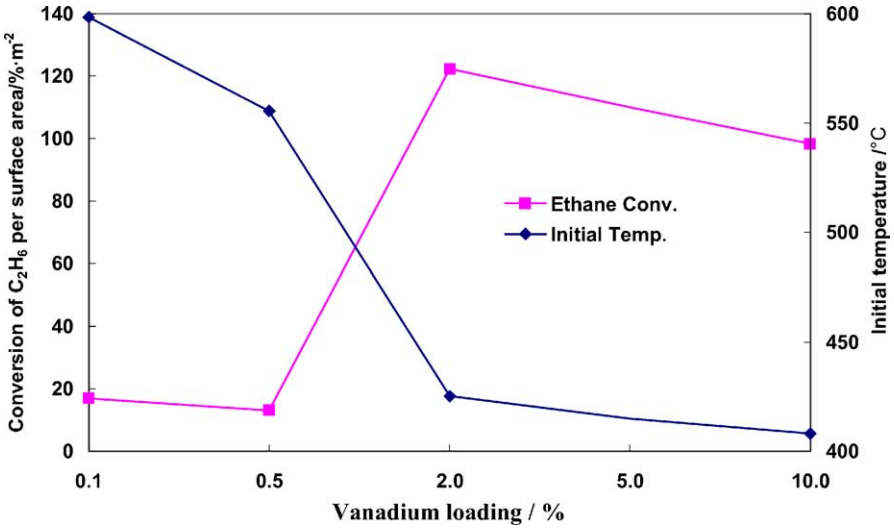

Fig. 9. Relation between ethane conversion per unit surface area of $Cs–V/SiO_2$ and its initial temperature in H_2-TPR. The reaction temperature for $C_2H_6 + O_2$ is 475 °C.

that acidity of catalyst favors the formation of ethylene from ethane over V/SiO_2.

4. Conclusions

(1) In both systems of V/SiO_2 (V:Si = *x*:Si) and $Cs–V/SiO_2$ (Cs:V:Si = 1:*x*:100), the reduction extent and the reducibility increase with the increasing of vanadium loading. The presence of cesium enhances the reduction extent. Only one reduction peak was observed on the samples with very low vanadium loading in which the isolated vanadyl species exist. This peak was mainly assigned to the reduction process of $V^{5+} \rightarrow V^{4+}$.

(2) The structures of vanadyl species have large effect on their reducibility. The reducibility order follows isolated vanadyl species < polymeric vanadyl species including microcrystalline vanadia.

(3) In the samples with high loading of vanadium (>2.0%), their reducibilities are high, thus the reducibility of the catalysts is the one of the most important factors to govern their reactivity. In contrast, in the samples with low loading of vanadium (<1.0%) or no, their reducibilities are low. Moreover, their reducibility is not so different. Therefore, the other factors, for example, the basicity or acidity of catalyst except for the reducibility, should be the main factor to control the reactivities of these catalysts. In the presence of cesium, the samples (2.0

and 10.0%) whose reducibilities are very high, i.e., the oxygen mobilities of which are very high, are for deep oxidation of ethane. On the contrary, the samples whose reducibilities are low are for the selective oxidation of ethane including ODH of ethane and the oxygenate formation. The reducibility of supported catalysts not only relates to their reactivity, but also controls the product distribution in some cases.

Acknowledgements

We acknowledge financial support of New Energy and Industrial Technology Development Organization (NEDO) of Japan. Zhen Zhao was supported by a Fellowship from NEDO. This work was partially supported by the National Science Foundation of China (20373043).

References

[1] D.B. Dadyburjor, S.S. Jewur, E. Ruckenstein, Catal. Rev.-Sci. Eng. 19 (1979) 293.
[2] Y. Moro-oka, Appl. Catal. A 181 (1999) 323.
[3] V.D. Sokolovskii, Catal. Today 24 (1995) 377.
[4] V.D. Sokolovskii, F. Arena, N. Giordano, A. Parmaliana, J. Catal. 167 (1997) 296.
[5] F. Cavani, F. Trifiro, Catal. Today 51 (1999) 561.
[6] G. Deo, I.E. Wachs, J. Catal. 129 (1991) 307.
[7] G. Deo, I.E. Wachs, J. Catal. 146 (1994) 323.
[8] T. Blasco, A. Galli, J.M.L. Nieto, J. Trifiro Catal. 169 (1997) 203.
[9] I.E. Wachs, B.M. Weckhuysen, Appl. Catal. 157 (1997) 67.
[10] A. Erdohelyi, F. Solymosi, J. Catal. 123 (1990) 31.
[11] X. Gao, S.R. Bare, J.L.G. Fierro, I.E. Wachs, J. Phys. Chem. B 103 (1999) 618.
[12] M.A. Eberhard, A. Proctor, M. Houalla, D.M. Hercules, J. Catal. 160 (1996) 27.
[13] V. Sokolovskii, F. Arena, S. Coluccia, A. Parmaliana, J. Catal. 173 (1998) 238.
[14] G.T. Went, L.-J. Leu, A.T. Bell, J. Catal. 134 (1992) 479.
[15] X. Gao, M.A. Banares, I.E. Wachs, J. Catal. 188 (1999) 325.
[16] F. Arena, F. Frusteri, A. Parmaliana, Appl. Catal. A 176 (1999) 189.
[17] Harber, A.J. Kozlowska, R. Kozlowski, J. Catal. 102 (1986) 52.
[18] M.M. Koranne, J.G. Goodwin, G. Marcelin, J. Catal. 148 (1994) 369.
[19] R. Grabowski, B. Grzybowska, A. Kozlowska, J. Sloczynski, K. Wcislo, Top. Catal. 3 (1996) 277.
[20] A. Galli, J.M.L. Nieto, A. Dejoz, M.I. Vazquez, Catal. Lett. 34 (1995) 51.
[21] L. Owens, H.H. Kung, J. Catal. 148 (1994) 587.
[22] G. Deo, I.E. Wachs, J. Catal. 146 (1994) 335.
[23] J. Zhu, S.L.T. Andersson, J. Chem. Soc., Farad. Trans. I 85 (1989) 3629.
[24] G.C. Bond, S.F. Tahir, Catal. Today 10 (1993) 393.
[25] M.G. Nobbenhuis, P. Hug, T. Mallat, A. Baiker, Appl. Catal. A 108 (1994) 241.
[26] R. Grabowski, B. Grzybowska, K. Samson, J. Sloczynski, J. Stoch, K. Wcislo, Appl. Catal. A 125 (1995) 129.
[27] A. Erdohelyi, F. Solymosi, J. Catal. 129 (1991) 497.
[28] A. Erdohelyi, F. Mate, F. Solymosi, J. Catal. 135 (1992) 563.
[29] D. Monti, A. Reller, A. Baiker, J. Catal. 93 (1985) 360.
[30] Klissurski, N. Abadzhijeva, React. Kinet. Catal. Lett. 2 (1975) 431.
[31] D. Miceli, F. Arena, A. Parmaliana, M.S. Scurrell, V. Sokolovskii, Catal. Lett. 18 (1993) 283.
[32] Y. Teng, T. Kobayashi, Chem. Lett. 327 (1998).
[33] Y. Teng, T. Kobayashi, Catal. Lett. 55 (1998) 33.
[34] K. Nakagawa, Y. Teng, Z. Zhao, Y. Yamada, A. Ueda, T. Suzuki, T. Kobayashi, Catal. Lett. 63 (1999) 79.
[35] Z. Zhao, Y. Yamada, A. Ueda, H. Sakurai, T. Kobayashi, Appl. Catal. A 196 (2000) 37.
[36] Z. Zhao, Y. Yamada, A. Ueda, T. Kobayashi, Shokubai (Catal. Catal.) 41 (1999) 435.
[37] Z. Zhao, Y. Yamada, Y. Teng, A. Ueda, K. Nakagawa, T. Kobayashi, J. Catal. 190 (2000) 215.
[38] Z. Zhao, T. Kobayashi, Appl. Catal. A 207 (2001) 139.
[39] T. Kobayashi, Catal. Today 71 (2001) 69.
[40] Z. Zhao, T. Kobayashi, I. E. Wachs, in preparation.